Study on the Connection of the Parking lots to Smart Grid Regarding Upgrade Synchronous Generator Performance

Mohammad Jafari [1,*] and Behzad Ahmadi [2]

1 Research Assistant at Materials and Energy Research Center (MERC), P.O. Box: 14155-4777, Tehran, Iran.
2 Power Electronics, Machines and Control Group, School of Electrical and Electronic Engineering, University of Nottingham, Nottingham, UK.
Corresponding author: m.jafari@merc.ac.ir

Increasing uncertainty parameters in power systems have caused the system to require a controller in order to retain the stability at the time presence of renewable power plants and electric vehicles. In this research, sliding mode and feedback linearization controllers have been proposed to control parking lots in the field of reactive power and desired targets; those have been followed up, including improving the voltage profile, the performance of synchronous generators and wind power plant in the transient state by the application of this control Method. The proposed control method is simulated on the IEEE-9 Bus grid and the extent of achieving the desired targets is examined in the efficiency of parking in the field of reactive power. The codes have been expanding by using MATLAB open source code software. Hence, the system developed by modelling the simulation results of this method indicates proper tracking of the control objectives in the normal grid conditions and the parking resistance of the transient States. It can be concluded that the presence of all-Electric Vehicles (parking lots) in the grid causes a reduction of roughly 50% in the rotor speed fluctuations of synchronous generators and reduces voltage fluctuations by up to 10 times by the qualitative and quantitative aspects, which indicates a 7.4% improvement in voltage profile. Therefore, by maintaining the grid voltage in the appropriate range and limiting the current flow in rotor windings, has been avoided the possibility of damage to the rotor winding during a probable short circuit in the grid.

Keywords: Nonlinear controller; Smart parking; Doubly fed induction generator; Sliding mode controller; feedback linearization controller.

http://dx.doi.org/10.22109 jemt.2019.160390.1144

Nomenclature

CT	Communication technology
IT	Information technology
EV	Electric Vehicle
V2G	Vehicle-To-Grid
SoC	State of Charge
IGBT	Insulated-gate bipolar transistor
L	Inductance of the connection cable
V_{Pccd}	Real component of the bus voltage connection of the V2G
V_{Pccq}	Imaginary component of the bus voltage connection of the V2G
V_{cd}	Real component of the internal voltage of the EV
V_{cq}	Imaginary component of the internal voltage of the EV
P_{PCC}	Active power injection to grid by EV
I_{sd}	Real current injection to grid by EV
Q_{PCC}	Reactive power injection to grid by EV
I_{Sq}	Imaginary current injection to grid by EV
$S_{P_{Pcc}}$	Sliding surface of active power
$S_{Q_{Pcc}}$	Sliding surface of active power
Kp	Positive integer coefficient
KQ	Positive integer coefficient
PEV	Plug in electrical vehicle
SMC	Sliding mode control
IOFC	Input - Output Feedback Linearization Controller
DFIG	Doubly fed induction generator
Pu	Per-unit

1. Introduction

Considering that in many countries, such as the United States, smart grid research has been notified to energy organizations as a rule and research budgets are defined, this grid is introduced as a new challenge to the electrical industry. According to the United-States-Energy-Organization, the smart grid is an automated power distribution grid in which electrical power transmission and exchange of information are carried out bilaterally. The grid has the ability to monitor and respond to any changes, by the sources of production to consumers and even to individual equipment. Therefore, the concept of smart grid and smart control (with proper communication protocol) represents a novel technology to the power supply of the electric vehicles and the greater penetration of renewable energy into the grid [1]. In other words, the smart grid provides a solution to solve the current grid challenges include of: 1- Reliability, 2- Environmental aspects and economical balances and 3- Energy efficiency as shown in Figure 1 [2].
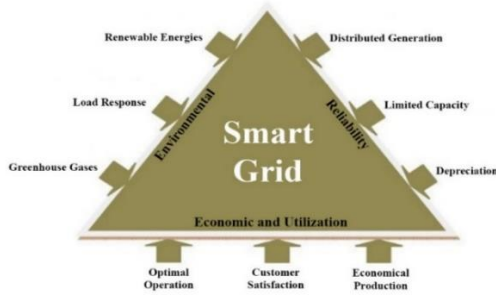

Fig. 1. Issues facing the smart grid [2].

As indicated in Figure 1, the presence and use of dispersed generation sources (including wind power plants with induction generators) play a very important role in the implementation of the intended purposes for an intelligent grid, both with the aim of to reduce pollution and greenhouse gases and to increase the efficiency and reliability of the power grid. While these dispersed generation, sources have proper reliability and can maintain their sustainability in critical grid conditions. Nevertheless, more importantly, by assuming smart grid, these devices can be used as active and reactive dynamic power resources and can be observed the impact of these vehicles on distributed generation sources, especially in times of crisis within the grid [3]. EVs can charge their batteries at any location in the parking position, such as parking lots or charging stations. Many researchers have studied concerning establishing the location of a parking lot or Plug-in Electrical Vehicle (PEV) charging stations. The Vehicle-To-Grid Connection (V2G) provides an excellent opportunity to design a two-way charger with the same function as an active filter for power grids. V2Gs can provide services such as rotation booking, regulator, renewable resources storage, and reactive power compensator to enhance grid power [4]. Therefore, V2Gs should store at least a percentage of their battery power daily to use this amount of energy to a daily mileage. Various studies have shown that vehicles are on average about 22 hours a day in park condition. Thus, during these 22 hours, they can be connected to the grid and be used as energy storage with their batteries [5]. The EVs energy storage capacity varies from 1 kWh to 30 kWh. However, fuel cell vehicles have more storage capacity [5]. The batteries have a fast response and can achieve the highest output in less than a millisecond. Such rapid responses cannot be achieved at any of the fast start-up power plants, which this feature makes them as an ideal option due to apply in the frequency setting process [6]. When the vehicle is in the mode of receiving energy from the grid, State of Charge (SoC) is rising, and SoC is declining when the vehicle is consuming energy. Figure 2 shows the SoC change process for a V2G in a typical day that charges the battery at home. In the presence of the vehicle in the parking lot, assuming it does not connect to the grid, the SoC remains stable. When returning from work to home, energy is used and SoC is increased. As noted above, each V2G must have a minimum of SoC to transport when leaving the parking lot [3]. While parking can be connected to the power grid, the SoC change process may be as shown in Figure 3. This Figure indicates that the parking consumes a vehicle battery and charges it and discharges it [5].
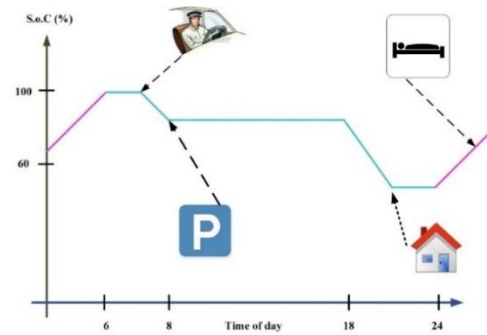

Fig. 2. The SoC change process for an EV in a typical day that charge battery at home [7]
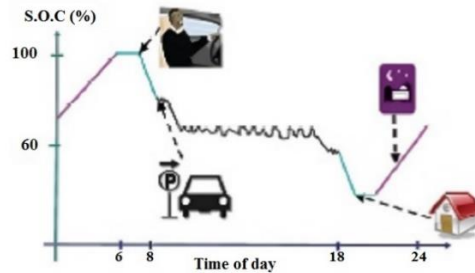

Fig. 3. SoC changes for an EV in a typical day while parking can be connected to the power grid [5]

By receiving and injecting the power at proper times, the distance between the maximum and minimum consumption can be significantly reduced. Figure 4 shows the use of V2Gs at peak times as generators and applying them as a load in non-courier hours, which can dramatically decrease the distance between the maximum and minimum load curves [8]. Nevertheless, EVs are generally connected to power distribution grids. In this research, the impact of vehicles on power grids has been evaluated. Therefore, integrating V2Gs and using them as a large storage system can examine their impact on power grids.
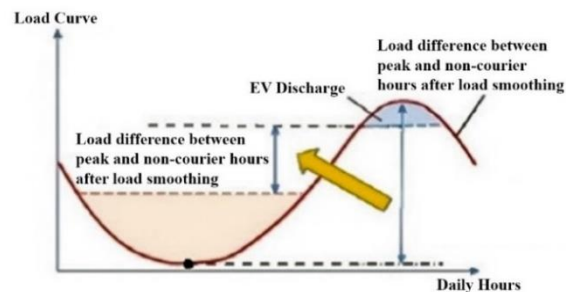

Fig. 4. Effects of V2Gs on load profile change [7]

In this research, by assuming 100% presence of communication technologies (CT) and information technologies (IT) in the power grid, it examines the services that EVs provide in the field of reactive power to the grid.

The main purpose of this article is to improve the grid status and the performance of wind power plants by utilizing the potential of EVs and using two nonlinear controller models. In previous studies, the presence of the car in the grid has been studied and those are evaluated by the technical and economic benefits [7]. Tabatabai et al. have investigated the economic calculations of EVs and their effect on improving the frequency of the grid. They found that by designing a system optimization algorithm would have able to intelligent planning for power plants, managing the consumption of electricity and use of EVs. In addition, by increasing grid reliability, the power would be saved whereas reduces the load on distribution grids and reduce the total cost of production [3].

The classic 9-bus system is the simplest model uses in dynamic power system studies and requires a minimum amount of data. For this purpose, Prakash and Tripathi studied the analysis of 9-bus multifunctional power systems, performed by using the power system stabilizer developed in MATLAB open source code software. By comparing the stability function of a multifunctional system and comparing the error-free results with the three-phase error in the power system (with a stabilizer), they found that transient stability of the system after 3.7 seconds is compensated. In the implementation of the PSS, the device obtained a better response in term of power swing compared with initial conditions [9]. Regarding previous researches, it is necessary to consider the presence of electric vehicles in a power grid for reducing network fluctuations and their positive impact on distributed generation plants.

In this research, the presence of the total number of EVs or smart parking in the IEEE-9 bus in the power grid has been studied more precisely. Generally, two main objectives have been applied by designing two nonlinear controllers (sliding mode controller and input-output feedback linearization controller) for smart parking as follows:

1- Investigate the effect of intelligent parking linking to the Bus (5) IEEE-9 bus system, as the weakest Bus for improving the speed and angle of the rotor of the synchronous generators. This cause increasing the transmission lines capacity and finally improving the grid voltage profile.

2- Protecting wind generators against unwanted or potential errors occurring in the grid and thereby reducing the voltage drop of terminal generators by providing reactive power to EVs.

In the final section, the simulation and results of the IEEE-9 Bus grid simulation are presented in two separate scenarios that mentioned above.

2. An electrical model of EV

As discussed earlier, the purpose of this paper is to examine the effect of total EVs in parking, on the power grid. Hence, the modeling of these cars has been neglected and EV parking lot has been applied like a large storage system in order to inject power to the grid and receive power. Therefore, only using a mathematical model presented in [10], [11], will be designed the appropriate controller for achieving the goals for this new storage system. The two-axis relation governing on EVs in a grid synchronous device is expressed as a Pu:

$$V_{cd} = L\frac{dI_{sd}}{dt} + V_{PCCd} \tag{1}$$

$$V_{cq} = L\frac{dI_{sq}}{dt} + V_{PCCq} \tag{2}$$

In the equations (1) and (2), L, the inductance of the connection cable, V_{Pccd} and V_{Pccq} is the real and imaginary component of the bus voltage

connection of the vehicle to the grid whereas V_{cd} and V_{cq} are the real and imaginary component of the internal voltage of the EV. Furthermore, the mathematical relations governing the active and reactive power distribution of the EV to the grid at the PCC bus are as follows:

$$P_{PCC} = V_{PCCd}I_{Sd} + V_{PCCq}I_{Sq} \tag{3}$$

$$Q_{PCC} = V_{PCCq}I_{Sd} - V_{PCCd}I_{Sq} \tag{4}$$

Naturally, in order to have a positive impact on the grid, regarding the application of smart parking lots, it is necessary to consider a suitable controller for these devices that track induce objectives accurately. The utilization of EVs in this research is the injection of reactive power in different conditions of the grid, for which purpose two types of sliding mode controller. Furthermore, the input-output feedback linearization controller is used for proper control of EVs, in which the design of these two types of EV controllers is discussed in part 4.

3. Introduction of Nonlinear Controllers

In order to control and survey the studied systems (EVs and doubly fed induction generators), there are two non-linear sliding mode controllers and input-output feedback linearization controller keys; the following is a brief explanation of these two nonlinear controllers.

3.1. Sliding mode controller

It is obvious that a controller based on the idea of controlling the first-order systems (i.e. systems that are described by first-order differential equations), whether non-linear or indefinite, is much easier than general systems of n-order (i.e., systems described by n-order equations). Uncertainty parameters will increase by developing of the power system, applying the renewable energies and connecting the electric vehicles to the grid [12]. The sliding mode controller has a special sensitivity to uncertainty parameters, due to its closed loop response. This system can limit nonlinear disturbances by extending uncertainty modeling. Therefore, using this controller can be effective to achieve the objectives of the research.

3.2. Feedback Linearization Controller

The main idea of this method is to transform the nonlinear system dynamics into linear (fully or partially), so that linear control can be exerted. The feedback linearity can be summarized in a way that by eliminating nonlinearity of a nonlinear system in its simplest form so that the dynamics of the loop depend on the linear form. In other words, the idea of linearizing feedback is to eliminate nonlinearities and apply a desired linear dynamic, which can be applied for the bundle of nonlinear systems, which are an epithet of the conditional or conventional form of controllability.

4. Design EV controllers

4.1. Sliding mode Controller

To design a sliding mode controller in an EV, the sliding surfaces, as Equations (5) and (6) should be defined. The $S_{p_{Pcc}}$ and $S_{Q_{Pcc}}$ are slipping surfaces of the active and reactive power of the vehicles are in the bus connection to the grid, respectively and k_P and k_Q are positive integer coefficients. It is necessary to note that, since all the correlations provided for an EV in a grid synchronization device, the vertical component of the voltage is zero and the horizontal component is constant. Control inputs (Vcd and Vcq) should be such that the derivative of the slip surfaces is zero (first method). Table 1 illustrates the relationship governing on the sliding mode controller design of smart parking lots (EV assembly).

Table 1. The relationship governing on the sliding mode controller design of smart parking lots.

Title	Equation	No.
sliding surface	$S_{P_{Pcc}} = e_{P_{Pcc}} + k_P \int e_{P_{Pcc}} dt$	**(5)**
	$e_{P_{Pcc}} = P_{Pcc\,ref} - P_{Pcc}$	**(6)**
A derivative of sliding surface	$\dot{s}_P = \dot{e}_P + k_P e_P$	**(7)**
	$\dot{s}_Q = \dot{e}_Q + k_Q e_Q$	**(8)**
	$\dot{P}_{pcc} = V_{PCCd}\dot{I}_{sd}$	**(9)**
	$\dot{Q}_{pcc} = -V_{PCCd}\dot{I}_{sq}$	**(10)**
	$\dot{s}_P = -\dfrac{V_{PCCd}{}^2}{L} + \dfrac{RV_{PCCd}I_{Sd}}{L} + \dfrac{V_{PCCd}V_{cd}}{L} + k_P e_P$	**(11)**
	$\dot{s}_Q = -\dfrac{RV_{PCCd}I_{Sq}}{L} - \dfrac{V_{PCCd}V_{cq}}{L} + k_Q e_Q$	**(12)**
	$\begin{bmatrix}\dot{S}_P\\\dot{S}_Q\end{bmatrix} = \begin{bmatrix}F_1\\F_2\end{bmatrix} - \begin{bmatrix}\dfrac{-V_{PCCd}}{L} & 0 \\ 0 & \dfrac{V_{PCCd}}{L}\end{bmatrix}\begin{bmatrix}V_{cd}\\V_{cq}\end{bmatrix}$	**(13)**
	$F_1 = -\dfrac{V_{PCCd}{}^2}{L} + \dfrac{RV_{PCCd}I_{Sd}}{L} + k_P e_P$	**(14)**
	$F_2 = -\dfrac{RV_{PCCd}I_{Sq}}{L} + k_Q e_Q$	**(15)**
Control Inputs	$\begin{bmatrix}V_{cd}\\V_{cq}\end{bmatrix} = D^{-1}\left(\begin{bmatrix}k_1 sgn(S_P)\\k_2 sgn(S_Q)\end{bmatrix} + \begin{bmatrix}F_1\\F_2\end{bmatrix}\right)$	**(16)**
	$D = \begin{bmatrix}\dfrac{-V_{PCCd}}{L} & 0 \\ 0 & \dfrac{V_{PCCd}}{L}\end{bmatrix}$	**(17)**

4.2. Input - Output Feedback Linearization Controller of EVs

As seen in the previous section, in control of EVs based on sliding mode controller, active and reactive power control of these vehicles has been considered. This section also has control objectives similar to the previous one. Therefore, design steps of the input-output feedback linearization controller as described above are done. The relation governing on the input-output feedback linearization controller design of EV parking lot is shown in Table 2.

Table 2. The relation governing on the input-output feedback linearization controller design of EV parking lot.

Equation	No.
$\dot{P}_{pcc} = V_{PCCd}\dot{I}_{sd}$	**(18)**
$\dot{Q}_{pcc} = -V_{PCCd}\dot{I}_{sq}$	**(19)**
$\dot{P}_{PCC} = -\dfrac{V_{PCCd}}{L}V_{cd} + F_P$	**(20)**
$\dot{Q}_{PCC} = \dfrac{V_{PCCd}}{L}V_{cq} + F_Q$	**(21)**
$F_P = \dfrac{V_{PCCd}}{L}(V_{PCCd} - RI_{Sd})$	**(22)**
$F_Q = -\dfrac{V_{PCCd}}{L}(-RI_{Sd})$	**(23)**
$V_{cd} = -\dfrac{L}{V_{PCCd}}(v_P - F_P)$	**(24)**
$V_{cq} = \dfrac{L}{V_{PCCd}}(v_Q - F_Q)$	**(25)**
$v_P = \dot{P}_{ref} - k_{P1}e_P - k_{P2}\int e_P dt,$ $e_P = P - P_{ref}$	**(26)**
$,v_Q = \dot{Q}_{ref} - k_{Q1}e_Q - k_{Q2}\int e_Q dt$ $e_Q = Q - Q_{ref}$	**(27)**

As seen in two previous part of this section, control inputs are designed for EVs by using two types of sliding mode controller and input-output linearization controller, which applying these inputs to the desired system (EV equations), the results can be observed.

5. Simulation and results

The purpose of this section is to examine the performance of these equipment and controllers designed for them in a standardized grid. Given this purpose, a standard IEEE-9 Bus grid is intended. By specifying the scenario, the method of adding this equipment to the grid and examining their performance in the standard grid is investigated and finally, the results of EVs performance assessment and wind power plants are presented in different scenarios. IEEE-9 Bus standard grid is a grid with three synchronous generators, three transformers and nine transmission lines. Information about generators, loads and transmission lines of this grid is given in reference [13]. A contributed single-line grid diagram is indicated in Figure 5.
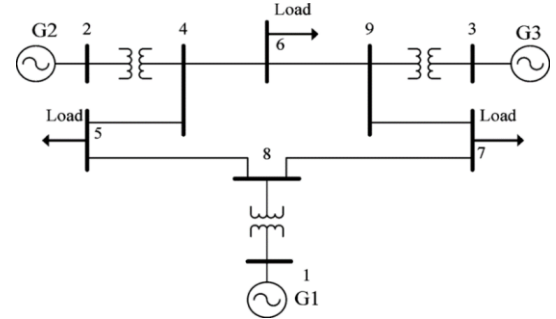

Fig. 5. The diagram of Single-Mode Standard IEEE-9 Bus system.

Reduced Admittance Matrix methods are used to solve the current, voltage, active and reactive power in this grid. Then, the governing equations on the grid are determined by applying this matrix. For this purpose, the load distribution analysis is performed on the grid by applying one of the Newton-Raphson and/or Gauss-Seidel methods. The results are based on load distribution that has been solved by initial conditions, time analysis of the grid equations and generator equations.

In the next step, the equations of the synchronous generators are implemented in the two-axis reference system of the grid synchronization. It should be noted that the generator (1) is a reference generator (Slack), also its voltage is always a Pu and its angle is zero. By these means, the mechanical equations of this generator are carried out. While the other two generators are the Real Power |*P*| and the Voltage Magnitude |*V*| (PV) generators, it is only determined the voltage and their active injection power whose amount is derived by the load-transfer analysis. As a result, the equations of generators (2) and (3) are fully simulated.

The grid equations can be solved by using the reduced admittance matrix after simulating the generators. Since the desired grid is a 9-bus system, the admittance matrix will be equal to equation (28) for this system .Table 3 shows the equivalent load admittance.

As shown in equation (28), the grid admittance matrix is a 9 × 9 square matrix. The first three columns and rows of this matrix are related to the generator bus (PV and Slack), and the next six rows and column are loaded bus {the Real Power |*P*| and Reactive Power |*Q*| (PQ)}. More ever, in order to implement this method, the equivalent load admittance in the grid should be obtained and add to the admittance matrix of the grid in the proper context.

Equation (29) shows the apparent power of each element in the power grid. Based on equation (31), the equivalent grid load admittance can be achieved with the apparent power and the size of the voltage bus which be connected to the consider load. Also, in equation (28), the adding equivalent admittance of each load to the admittance matrix of the system is obtained. In this method, if the load is on the bus i, the equivalent admittance will be added to it.

This process is performed to add all grid loads to the admittance matrix of the system. On the other hand, the voltage and current of all grid buses in the admittance equation grid (Equation (32)) should be applied. In this regard, power injection equipment (active or reactive) is modelled as a current source and in the bus where there is no power injection, the amount of this source is zero.

Regarding Equation (32) and the above-mentioned contents, I4 to I9 currents are zero because these buses are PQ and there is no power injection in this type of bus. V1 (reference bus voltage) is always equal to one Pu as well. Consequently, according to the above-presented content, the entries of the matrix i are zero after the fourth row. Therefore, can separate the bus equations of the power injection to the bus equations of the power non-injection. This can be performed by achieving the reduced admittance matrix.

A decreasing order matrix is a square matrix with three rows and columns because there are only three busses (1), (2) and (3) in 9 bus systems that do power injection to the system. If Y_{bus} is taken as Equation (33), the decreasing order matrix is calculated as Equation (34). After obtaining the reduced admittance matrix, the grid equations are given in Equation (35) in the bus that has power injection. Equation (35) is solved systematically by Fourth-Order Runge-Kutta method. In this way, the initial voltage of all the buses is determined by using the load distribution analysis. Therefore, I2 and I3 currents are obtained by placing V2 and V3 voltages in generator equations. Furthermore, the current I1 is achieved by multiplying the first row of the reduced admittance matrix in the voltage vector V1, V2 and V3.

By acquiring the currents and placing them in equation (35), the voltages can be calculated for the next step.

Table 3. Relations governing on the IEEE-9 Bus power system.

| Title	Equation	
GridAdmittance Matrix	$$Y_{bus} = \begin{bmatrix} Y_{11} & \cdots & Y_{19} \\ \vdots & \ddots & \vdots \\ Y_{91} & \cdots & Y_{99} \end{bmatrix}$$	(28)
Apparent Power	$S = VI^*$	(29)
Load Admittance	$I_{Load} = V_{Load} Y_{Load}$	(30)
	$$S_{Load} = V_{Load}(V_{Load}Y_{Load})^* = |V_{Load}|^2 Y_{Load}^* \rightarrow Y_{Load} = \frac{S_{Load}^*}{|V_{Load}|^2}$$	(31)
	$$\begin{bmatrix} I_1 \\ \vdots \\ I_9 \end{bmatrix} = \begin{bmatrix} Y_{11} & \cdots & Y_{19} \\ \vdots & \ddots & \vdots \\ Y_{91} & \cdots & Y_{99} \end{bmatrix}\begin{bmatrix} V_1 \\ \vdots \\ V_9 \end{bmatrix}$$	(32)
	$$Y_{bus} = \begin{bmatrix} Y_{11} & Y_{12} & Y_{13} & \vdots & Y_{14} & Y_{15} & Y_{16} & Y_{17} & Y_{18} & Y_{19} \\ Y_{21} & Y_{22} & Y_{23} & \vdots & Y_{24} & Y_{25} & Y_{26} & Y_{27} & Y_{28} & Y_{29} \\ Y_{31} & Y_{32} & Y_{33} & \vdots & Y_{34} & Y_{35} & Y_{36} & Y_{37} & Y_{38} & Y_{39} \\ \cdots & \cdots & \cdots & \cdots & \cdots & \cdots & \cdots & \cdots & \cdots \\ Y_{41} & Y_{42} & Y_{43} & \vdots & Y_{44} & Y_{45} & Y_{46} & Y_{47} & Y_{48} & Y_{49} \\ Y_{51} & Y_{52} & Y_{53} & \vdots & Y_{54} & Y_{55} & Y_{56} & Y_{57} & Y_{58} & Y_{59} \\ Y_{61} & Y_{62} & Y_{63} & \vdots & Y_{64} & Y_{65} & Y_{66} & Y_{67} & Y_{68} & Y_{69} \\ Y_{71} & Y_{72} & Y_{73} & \vdots & Y_{74} & Y_{75} & Y_{76} & Y_{77} & Y_{78} & Y_{79} \\ Y_{81} & Y_{82} & Y_{83} & \vdots & Y_{84} & Y_{85} & Y_{86} & Y_{87} & Y_{88} & Y_{89} \\ Y_{91} & Y_{92} & Y_{93} & \vdots & Y_{94} & Y_{95} & Y_{96} & Y_{97} & Y_{98} & Y_{99} \end{bmatrix} = \begin{bmatrix} A_1 & \vdots & A_2 \\ \cdots & \vdots & \cdots \\ A_3 & \vdots & A_4 \end{bmatrix}$$	(33)
	$Y_{redused} = A_1 - A_2 A_4^{-1} A_3$	(34)
	$$\begin{bmatrix} I_1 \\ I_2 \\ I_3 \end{bmatrix} = Y_{reduced}\begin{bmatrix} V_1 \\ V_2 \\ V_3 \end{bmatrix}$$	(35)
	$V_{PQ} = -A_4^{-1} A_3 V_{PV}$	(36)

Then, the currents can be achieved in the next step in accordance with the method described for the first step. The new values of the currents are placed in equation (35) and calculated the new step voltages (third step). This process continues up to the end of the simulation time. As a result, the injection current and the voltage of the bus with the power supply source are solved in accordance with equation (35). Moreover, to achieve the PQ bus voltage (without a power source) the relations (32) and (33) derived the following equation.

In Equation (36), VPV is the voltage vector of the generator bus (bus with power injection) and VPQ is the vector of load bus voltage (bus without power injection).

As a result, by applying the presented content the simulation of the IEEE-9 Bus standard system is taking place. Figure 6 illustrates the overview of this simulation in the MATLAB-Simulink open source code software. As shown in Figure 6, Gen 1, Gen 2 and Gen 3 blocks are the simulation results of the synchronous generator equations (1), (2) and (3) respectively, which is only simulated the mechanical equations of the synchronous generator (1) in the Gen 1 block and full-time equations of the generator (2) and (3) in the Gen 2 and Gen 3 blocks. Further intended an excitation system to have a voltage equal

to 1.025 Pu in terminal generators in the simulation of synchronous generators (2) and (3).

In the next sections, to better understanding the impact of equipment such as EVs and wind power plants on each other and grid parameters, the results of simulation of IEEE-9 Bus standard grid without the presence of this equipment are shown as follow.
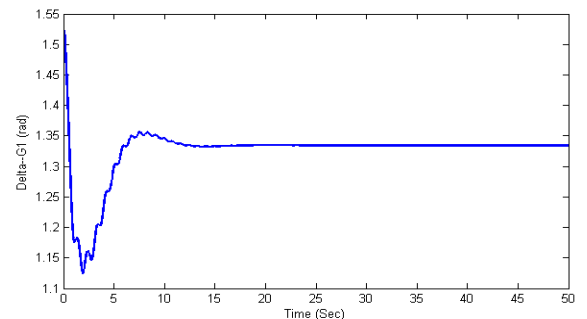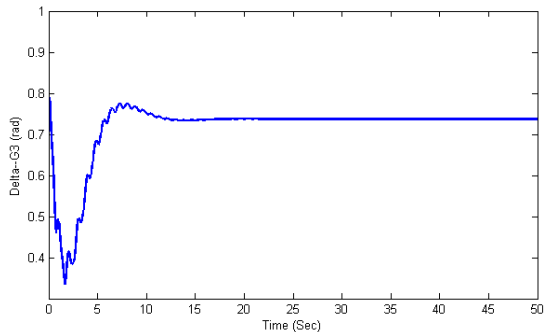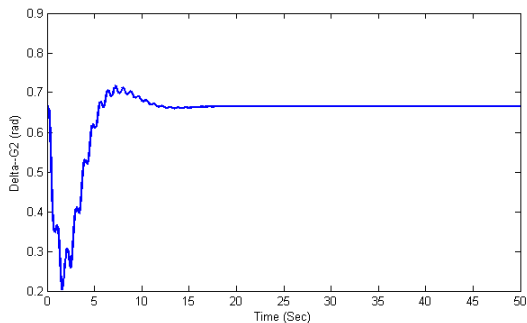
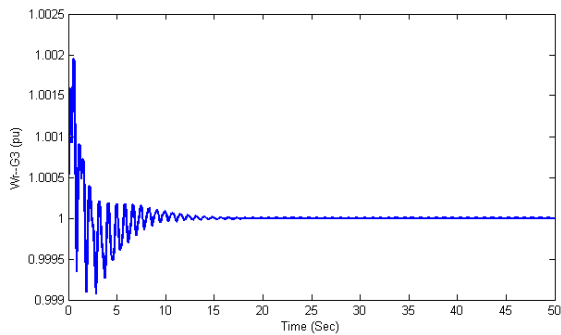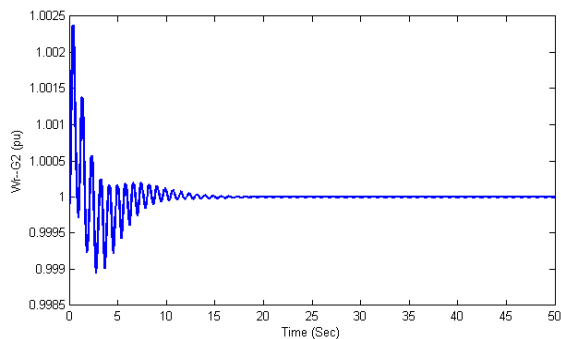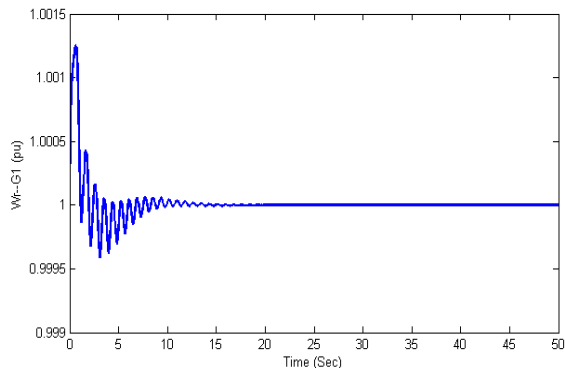**Fig. 6.** Diagram of the synchronous generator rotor angle (1, 2 and 3) VS time.

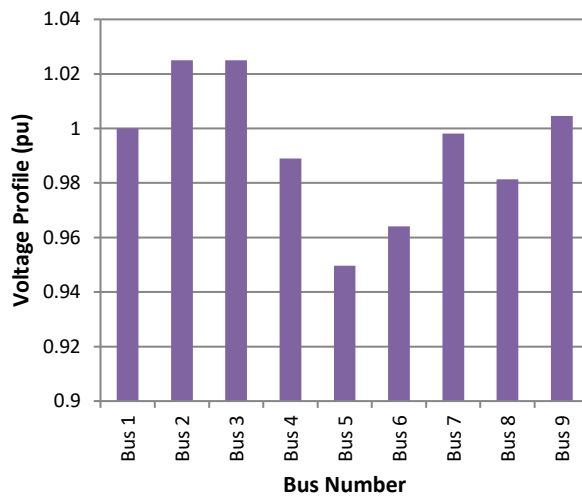**Fig. 7.** Diagram of the synchronous generator rotor speed (1, 2 and 3) VS time.

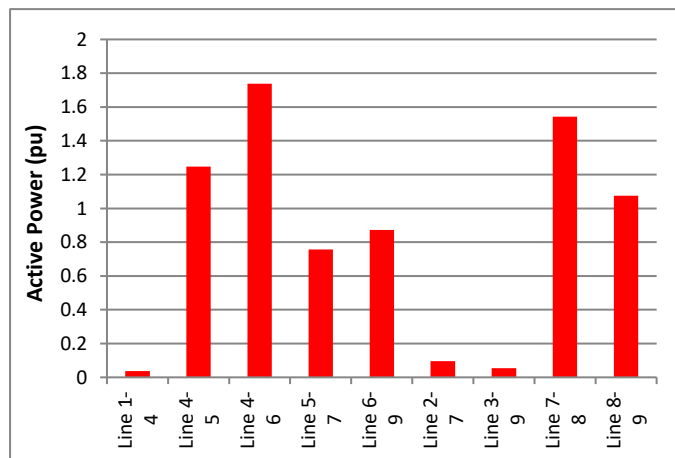**Fig. 8.** Bar diagram of the bus voltage profile according to the bus number.

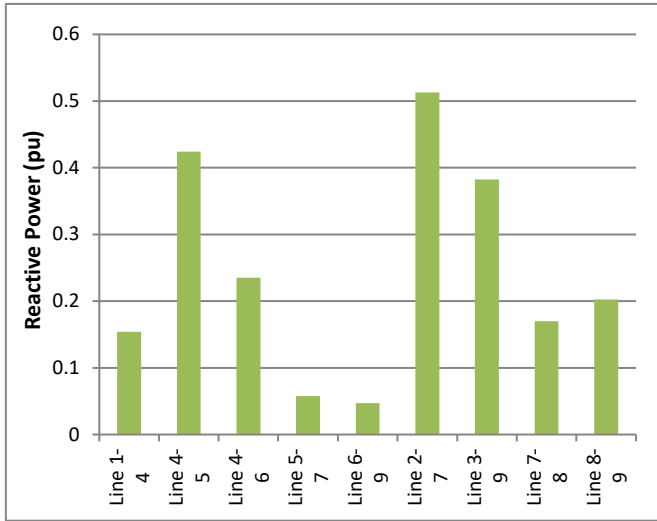**Fig. 9.** Bar diagram of the transit active power in lines according to the line number.

Fig. 10. Bar diagram of the transit reactive power in lines according to the line number.

5.1. Effect of EVs on improving the bus voltage profile of the IEEE-9 Bus standard grid

By assuming EVs as a smart park, most of these positive impacts on power balance, include: grid demand response, preventing the power valleys in the grid, assessing grid with distributed generation sources, such as wind power plants. In the other hand, within the recent studies, more attention has been devoted to the analysis of the participation of EVs in active power transmission, which would allow the charging and discharge of EVs within certain and planned hours. Meanwhile, by the same assumption of the smart park of EVs, the aim is to investigate the effect of this equipment on the 9-bus grid during the injection of reactive power to the grid (with and without the presence of a wind power plant). Therefore, in this case, EVs do not need to be recharged and discharged, as mentioned before.

By connecting a smart parking set of EVs to the grid the single-line diagram of the grid in the new mode is shown in Figure 11.
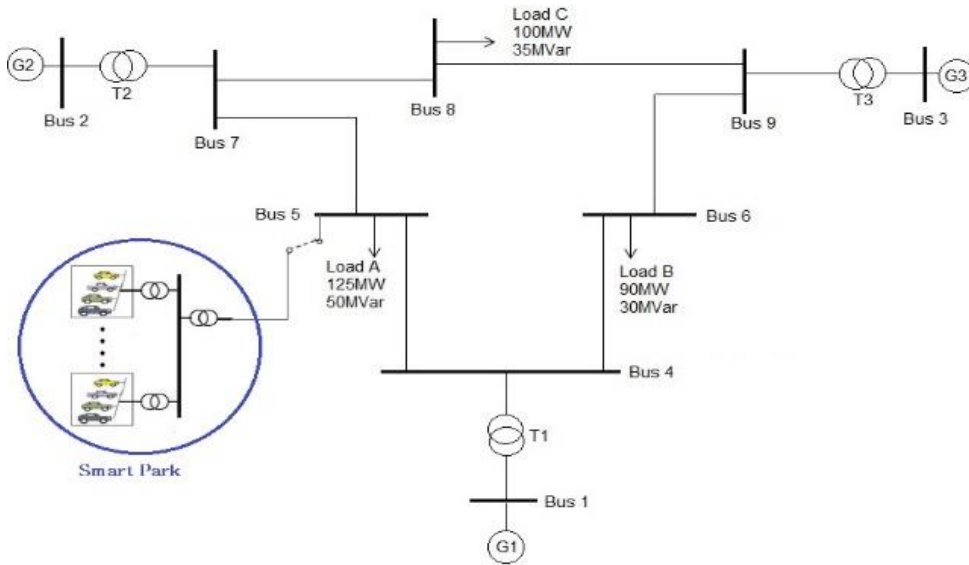

Fig. 11. Single-line Diagram of IEEE-9 Bus standard grid in the smart park connection mode to the grid

As illustrated in Figure 5, a set smart parks is connected to the grid on the bus (5). Based on the load analysis, the reason for connecting this set to the grid in this bus is that the bus (5) is the weakest bus in terms of the size of the voltage.

Based on governing equations and control signals on EVs that can simulate these vehicles, it is necessary to note that in each controller, is needed to determine the reference value of the active (P_{Ref}) and reactive (Q_{Ref}) power units of the EV to the grid. The determination of these two parameters is the consideration of the reference active power (P_{Ref}) equal to zero, so that the EVs are only involved in the transmission of reactive power. In other words, EVs do not require buying recharge by the grid due to their contribution to improving grid status. The reference reactive power (Q_{Ref}) is defined as the block diagram in Figure 12.
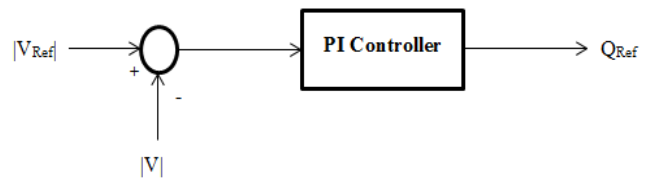

Fig. 12. Block Diagram of reactive power reference with the aim of controlling the size of the bus voltage of connecting EV to the grid.

As shown in Figure 12, in order to determine the reference reactive power for nonlinear controllers used in the control of the EV, Initially the size of the vehicle bus connection to the bus (5) should be measured. As shown in Figure 12, in order to determine the reference reactive power for nonlinear controllers used in the control of the EV, Initially the size of the vehicle bus connection to the bus (5) should be measured. Then it is compared with the reference voltage value, which

considered within the simulation equal to 1.02 Pu and passes through a PI controller. The output of the PI controller will deliver the reactive power to the nonlinear controllers.

Regarding the above-mentioned contents and the implementation of the simulations, the results of connecting EV with a sliding mode controller to the bus (5) are presented in the 9-bus system. In this case, EVs are controlled in order to control the bus voltage (5). These controller results are completely comparable and the diagram of them are coincident accurately.
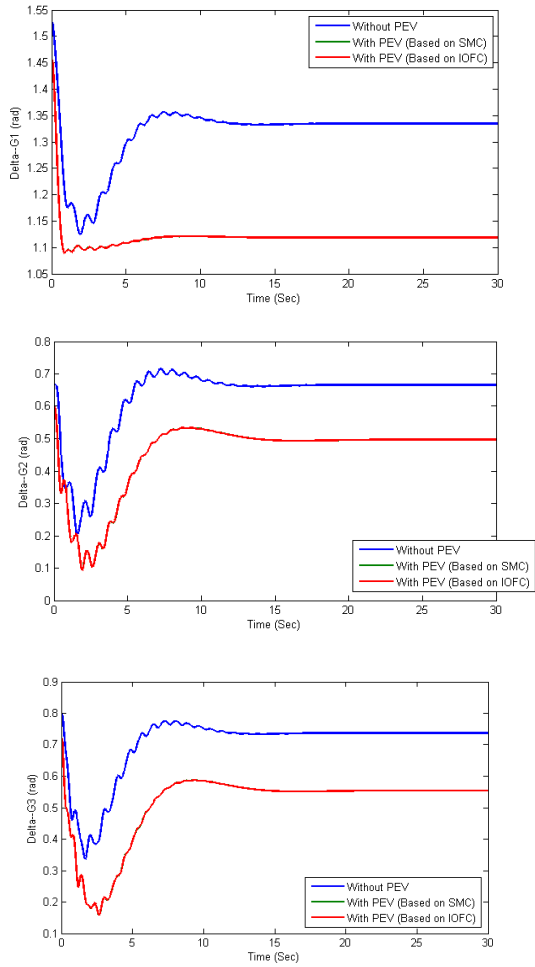

Fig. 13. The diagram of synchronous generator rotor angle (1, 2, 3) with the presence and the absence of EV at the bus (5) VS time (based on the sliding mode controller and input-output feedback linearization controller).
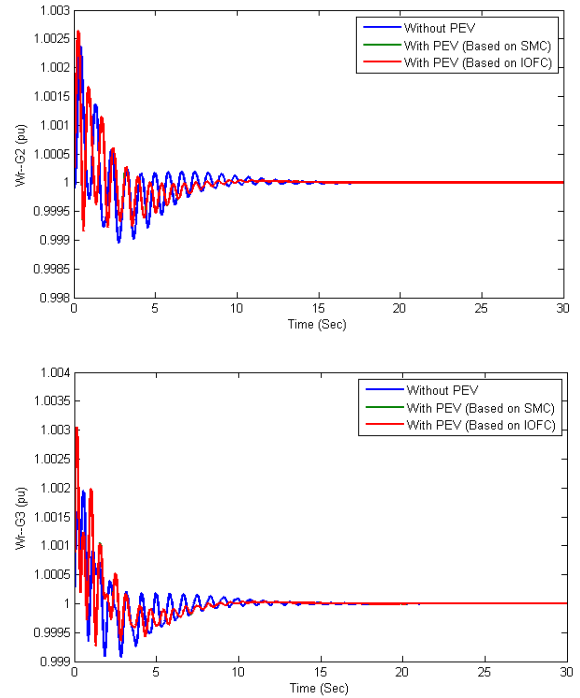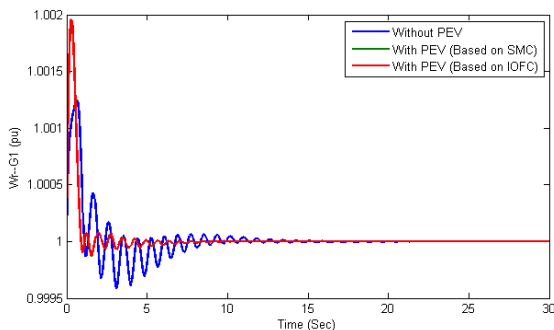

Fig. 14. The diagram of synchronous generator rotor speed (1, 2, 3) with the presence and the absence of EV at the bus (5) VS time (based on the sliding mode controller and input-output feedback linearization controller).

Forasmuch as the bus voltage profile of the grid bus is the same in both control methods (Figure 15), the active and reactive power transmissions in the lines are the same in both methods. Figure 16 indicates the bar diagram of the transitional active and reactive power lines based on the sliding mode controller and Figure 17 shows the bus voltage (5) in the transient state regarding both controllers of the sliding mode controller and input-output feedback linearization controller on both presence and absence of EVs.
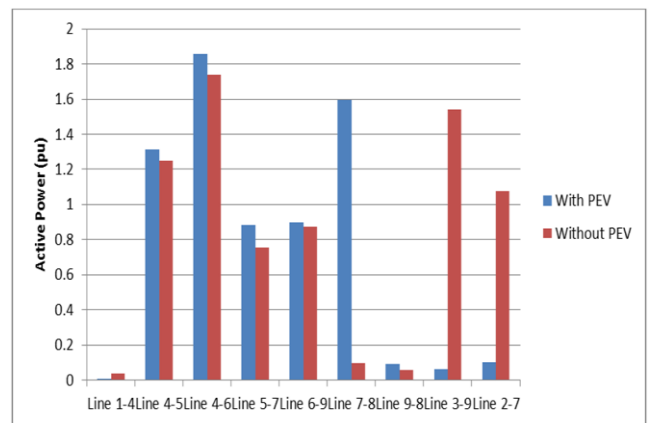

Fig. 15. Active power bar diagram that passing through the lines in two modes of presence and absence of EVs in the bus (5).
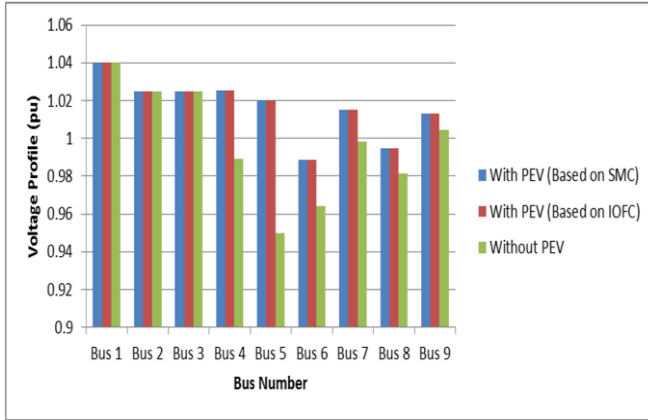
Fig. 16. The bus voltage profile in two modes of presence and absence of EVs in the bus (5).
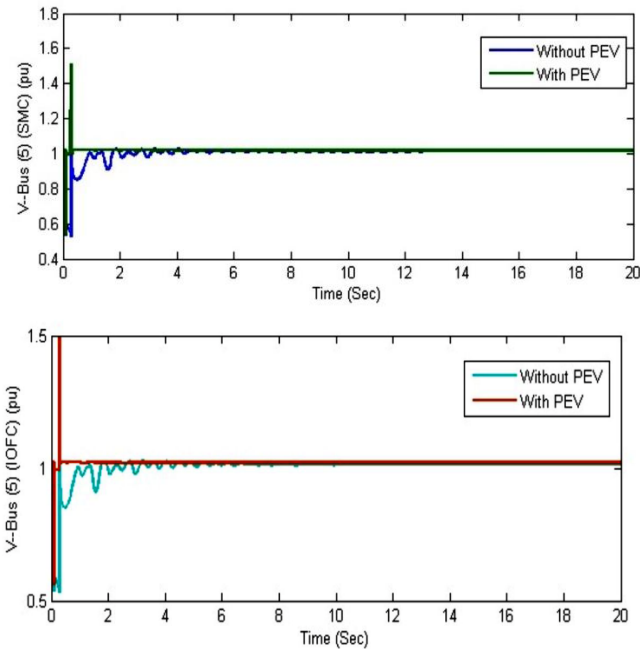

Fig. 17. Voltage diagram of the bus (5) in a transient state with the presence and absence of EVs VS time (based on the sliding mode controller and input-output feedback linearization controller)

As observed in the Figures (15 to 17), with the presence of EVs on the bus (5), the voltage of bus (5) increased from 0.9497 Pu to the desired value of 1.02 Pu, which satisfied the main purpose of this scenario.

5.2. Effect of EVs on wind power plant by doubly fed induction generator in the transient state

In this section, intended to examine the effect of these vehicles in the transient state of the doubly fed induction generator by employing EVs at the bus connection of the wind power plant to the grid (by the same purpose as in the previous section). Hence, DFIG has been selected for this purpose, whose benefits are greater than the count of its various parts. Other advantages of these types of turbines include the use of variable speed DFIG wind turbine based on active power and reactive power capabilities, lower cost converter and power losses compared to wind turbine by applying a constant

speed generator. Additional information on DFIG is given in [14].

By simulating regards to this scenario, 2 MW wind power plant is to be connected to the 9-bus grid at the bus (5). As a result, the new power injector, which is supposed to be added to the grid is similar to the addition of PEVs in the previous section. In the following, the results of the 9-bus grid simulation by the presence of a wind power plant with a doubly fed induction generator are shown in Figures 18 and 19, in the absence of any turbulence in the grid.
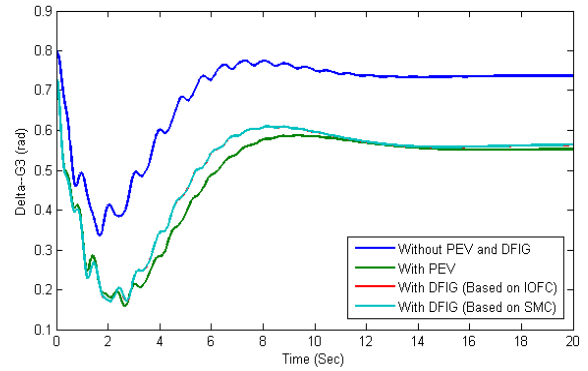

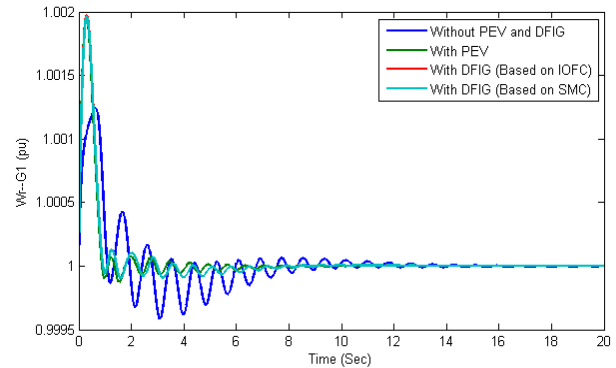**Fig. 18.** diagram of the synchronous generator rotor angle in time

Fig. 19. diagram of synchronous generator rotor speed (1) in time

6. Conclusion

In this paper by assuming the presence of telecommunication and information infrastructures, which require the transition from traditional power grids and the transformation of these grids into smart grids, the impact of integrated EVs (Smart Park) and vehicle to grid connection (V2G) in the reactive power has been studied. These vehicles have been contributed to the transfer of reactive power to the grid in the monitoring and flexibility of a sample smart grid. In other words, there is no active power between these parking lots and the grid. Therefore, these vehicles do not interfere in grid load and their charging schedule when used in the field of reactive power and this is an important advantage. In other words, these parking lots can play a role in supplying reactive power at these times such as the parallel Facts.

Regard to improving the profile of grid bus voltage, the following results are achieved:

1. By placing a Smart Park in the weakest bus of the grid in terms of the voltage (Bus (5)), the voltage has improved to 1.02 Pu.

2. The rotor speed fluctuations of the synchronous generators in the grid is reduced by providing reactive power through the smart park

connected to the bus (5).

3. With the presence of EVs in the bus (5), the capacity of the lines has increased and hence the transmission power in the lines has increased too. Thereby the losses of the studied power system has reduced.

Furthermore, by applying this method, can supply reactive power of wind power plant can be supplied by doubly fed induction generator in a transient state, which the following results are gained by examining the effect of EVs on the grid with the presence of wind turbines and using these controllers:

1. By placing a smart park at the bus connection of the wind power plant to the power bus (5) and the presence of a short circuit error of 200 milliseconds in the bus bar line (5) and (7), the voltage drop of the Induction generator terminal is less than the case when EVs are not connected.

2. The transient flow generated in the rotor windings is very limited due to the decrease in the voltage drop of the generator terminal to supply reactive power through PEVs and the preserve of the voltage of the bus (5) in the proper range and prevent the possibility of damage to the rotor coils during short circuit periods.

3. In addition to preventing the passage of a dangerous flow of rotor coils, with the presence of the smart park in the bus (5), other parts of the induction generator, like the DC link voltage, had better situations than those vehicles are not a presence in the bus (5).

7. References

[1] Raoofat M., M. Saad, S. Lefebvre, D. Asber, H. Mehrjedri and L. Lenoir, "Wind power smoothing using demand response of electric vehicle,es", *Electrical Power and Energy Systems* 99 (2018) 164–174

[2] Arani, M. and I.Mohamed, "Cooperative Control of Wind Power Generator and Electric Vehicles for Microgrid Primary Frequency Regulation", *IEEE Transactions on Smart Grid* 2017

[3] Tabatabaee, S., S. S. Mortazavi, T. Niknam, "Stochastic Scheduling of Local Distribution Systems Considering High Penetration of Plug-in Electric Vehicles and Renewable Energy Sources", *Energy* (2016),

[4] Khan, A., S. Memon and T.P. Sattar, "Analyzing Integrated Renewable Energy and Smart-Grid Systems to Improve Voltage Quality and Harmonic Distortion Losses at Electric-Vehicle Charging Stations", *IEEE Access*, 2018(6), 26404-26416

[5] Rong Yu, W. Z., Sh. Xie, Y. Zhang, K. Y. Yau, "On Stability and Robustness of Demand Response in V2G Mobile Energy Networks", *IEEE Transactions on Smart Grid*, 2016

[6] Stroe, D., V. Knap, M. Swierczynski, A. Stroe, R. Teodorescu, "Operation of Grid-Connected Lithium-Ion Battery Energy Storage System for Primary Frequency Regulation: A Battery Lifetime Perspective", *IEEE Transactions on Industry Applications*, 2016

[7] Rahbari O., Vafaeipour M, Omar N, Rosen MA, Hegazy O, Timmermans J-M,Heibati M, Bossche PVD, "An optimal versatile control approach for plug-in electric vehicles to integrate renewable energy sources and smart grids", *Energy* (2017)

[8] Inage, S., "Modelling Load Shifting Using Electric Vehicles in a Smart Grid Environment " *IEA Energy Papers*, 2010.

[9] Prakash, D. and v, k, Tripathi, "Enhancing Stability of Multi-Machine IEEE 9 Bus Power System Network Using PSS", *International Journal of Advanced Research in Electrical, Electronics and Instrumentation Engineering*, Vol. 4, Issue 5, May 2015.

[10] Mitra, P., Venayagamoorthy, G.K., Corzine, K.A., "SmartPark as a Virtual STATCOM," Smart Grid, *IEEE Transactions* on vol. 2. no.3, pp. 445,455. 2011.

[11] Ayoubia, Y., M. Elsied, A. Oukaour, H. Chaoui, Y. Slamani, H. Gualous, "Four-phase interleaved DC/DC boost converter interfaces forsuper-capacitors in electric vehicle application based onadvancedsliding mode control design", *Electric Power Systems Research* 134 (2016) 186–196

[12] Soroudi, A., T. Amraee, "Decision making under uncertainty in energy systems: State of the art", *Renewable and Sustainable Energy Reviews* 28 (2013) 376–384

[13] Asija. D., P. Choudekar, Ruchira, M. Chouhan, "Performance Evaluation and Improvement in Transient Instability of IEEE 9 bus System using exciter and governor control", *Procedia Computer Science* 70 (2015) 733 – 739.

[14] Kaloi, Gh.S., J. Wang, M.H. Baloch, "Active and reactive power control of the doubly fed induction generator based on wind energy conversion system", *Energy Reports* 2 (2016) 194–200.